Research Square

Preprints are preliminary reports that have not undergone peer review.
They should not be considered conclusive, used to inform clinical practice,
or referenced by the media as validated information.

Effect of Annealing Temperature on Mechanical Properties, Texture and Recrystallization Kinetics of Cold-Rolled Thin Sheet of Al–Mg Alloy

Ivan D. Pospelov

idpospelov@chsu.ru

Cherepovets State University https://orcid.org/0009-0000-5974-5718

Andrey A. Nikiforov

Cherepovets State University https://orcid.org/0009-0005-8404-7694

Natalia L. Bolobanova

Cherepovets State University https://orcid.org/0000-0003-1243-7173

Sergey A. Pyatkovsky

Cherepovets State University https://orcid.org/0009-0001-3157-1047

Zoya M. Malkova

Cherepovets State University https://orcid.org/0009-0009-6403-2996

Research Article

Keywords: Al–Mg alloy, Mechanical properties, Regression equations, Texture, Recrystallization kinetics

Posted Date: June 16th, 2026

DOI: https://doi.org/10.21203/rs.3.rs-10015646/v1

License: This work is licensed under a Creative Commons Attribution 4.0 International License.
Read Full License

Additional Declarations: The authors declare no competing interests.

Effect of Annealing Temperature on Mechanical Properties, Texture and Recrystallization Kinetics of Cold-Rolled Thin Sheet of Al–Mg Alloy

Ivan D. Pospelov ORCID: 0009-0000-5974-5718[1*], Andrey A. Nikiforov ORCID: 0009-0005-8404-7694[2†], Natalia L. Bolobanova ORCID: 0000-0003-1243-7173[1†], Sergey A. Pyatkovsky ORCID: 0009-0001-3157-1047[1,2†], Zoya M. Malkova ORCID: 0009-0009-6403-2996[2†]

[1*]Department of Metallurgy, Mechanical Engineering and Technological Equipment, Cherepovets State University, 5 Lunacharsky Ave., Cherepovets, 162600, Vologda oblast, Russia.

[2]Research Laboratory "Materials Science and Functional Materials" of the Advanced Engineering School, Cherepovets State University, 5 Lunacharsky Ave., Cherepovets, 162600, Vologda oblast, Russia.

*Corresponding author(s). E-mail(s): idpospelov@chsu.ru;
Contributing authors: aanikiforov1@chsu.ru; nlbolobanova@chsu.ru; sapiatkovskii2@chsu.ru; zmmalkova@chsu.ru;
†These authors contributed equally to this work.

Abstract

To obtain the specified mechanical properties of aluminum-magnesium alloys, controlled annealing of cold-rolled sheets is required. Despite numerous studies on the recrystallization of Al–Mg alloys, the very early stages of the process remain unclear, especially in the commercial AA5056 alloy (ANSI H35.2) with high magnesium content. The aim of this work is to establish the effect of annealing temperature on the mechanical properties, texture, and primary recrystallization kinetics of a cold-rolled AA5056 alloy sheet. The research methods included static tensile testing according to ISO 6892-1:2019, texture analysis by the inverse pole figure method with Morris normalization for ten reflections of the face-centered cubic (FCC) lattice, and the X-ray photographic method of recording Debye patterns in a back-reflection camera using CuKα radiation. Based on these methods, a qualitative and quantitative assessment of the changes in mechanical properties, texture evolution, and the onset of recrystallization (manifested by the appearance of spotty reflections on the (511) and (422) Debye rings) was carried out. It was found that with increasing annealing temperature, the ultimate tensile strength and yield strength regularly decrease, while the elongation increases. Regression equations describing these dependences were obtained. In the cold-rolled state and after annealing up to 390 ℃, the maximum pole density in the inverse pole figures corresponds to the <001> direction, which may be associated with the cube texture {100}<001>, while upon heating above 470 ℃ it is replaced by the {311}<211> and A/rot.W {511}<110> components. The appearance of spotty reflections at 370 ℃ indicates the onset of primary recrystallization. At 330 ℃, a local decrease in ductility is

observed, associated with the precipitation of a secondary phase. The obtained data make it possible to select annealing regimes for rolled sheets of Al-Mg alloys to achieve the required combination of strength and ductility, as well as to predict texture changes. The temperature of the onset of intensive recrystallization of AA5056 alloy is 370 ℃. The regression equations enable the calculation of mechanical properties in the studied temperature range. The cube texture persists up to 390 ℃, while above 470 ℃ the components of the deformation rolling texture dominate.

Keywords: Al–Mg alloy, Mechanical properties, Regression equations, Texture, Recrystallization kinetics

1 Introduction

Recrystallization annealing is a key heat treatment operation for deformed aluminum alloys, making it possible to control the set of mechanical properties and performance characteristics. Among the corrosion-resistant alloys of the Al–Mg system, AA5056 alloy occupies a special place because it is widely used in shipbuilding, automotive and chemical engineering due to its high corrosion resistance and satisfactory weldability. However, cold rolling of sheets made of this alloy leads to work hardening and the formation of a non-equilibrium microstructure, which requires subsequent annealing to restore ductility [1–4]. Controlling the recrystallization process is necessary to achieve a desired combination of strength and ductility, as well as to prevent undesirable grain growth.

The influence of magnesium on the recrystallization kinetics of aluminum is well known: magnesium increases the stacking fault energy, which accelerates polygonization, but at the same time retards recrystallization through a solute drag effect [5]. Moreover, Al–Mg alloys often contain manganese and other transition metals that form Al-Mn and α-Al(FeMn)Si intermetallics, which effectively suppress recrystallization [6–10]. In AA5056 alloy containing 5.8% Mg and 0.5% Mn, the combined effect of magnesium and manganese determines the complex evolution of the microstructure and texture during annealing [11–13]. Some features of recrystallization related to alloying with chromium, zirconium, scandium and lithium have also been studied [14–19].

Various methods are used to study recrystallization: light and electron microscopy, including polarized light [20], differential scanning calorimetry [5], hardness and electrical resistivity measurements [6], as well as X-ray methods [21–23]. Microscopic methods allow direct observation of the nucleation and growth of new grains; however, they are labor-intensive for quantitative assessment of the very early stages, when the recrystallized volume fraction does not exceed a few tenths of a percent. X-ray methods, in particular the X-ray photographic method of recording Debye patterns in a back-reflection camera [24], provide integral information over the entire sample area and make it possible to detect the appearance of spotty reflections from undistorted crystallites, which corresponds to the onset of primary recrystallization [25]. This method has been successfully applied to a number of alloys [3, 25], but systematic studies of recrystallization kinetics for AA5056 alloy using this method are lacking.

Despite the considerable number of works on recrystallization of aluminum-magnesium alloys, the following issues remain unresolved. First, the exact temperature of the onset of extensive recrystallization of cold-rolled AA5056 sheet at a moderate reduction of about 38% has not been established. Second, quantitative data on texture evolution in the narrow annealing temperature range of 330-390 ℃, where a change in the predominant orientations occurs, are absent. Third, the correlation between the change in the crystal lattice parameter due to solid solution decomposition and the local decrease in ductility observed in some works at temperatures around 330 ℃ has not been studied.

The aim of the present work is to establish the effect of recrystallization annealing temperature in the range of 290-530 ℃ with a hold of 1 hour on the mechanical properties, texture and primary recrystallization kinetics of a cold-rolled AA5056 alloy sheet.

To achieve this aim, the following tasks were addressed:

1. To determine the ultimate tensile strength, yield strength and elongation of samples after annealing at different temperatures and to obtain

regression equations for calculating these properties.

2. To investigate texture evolution by the inverse pole figure method and to identify the temperatures at which the predominant crystallographic orientations change.

3. To record the onset of primary recrystallization using the X-ray photographic method (appearance of spotty reflections on Debye rings) and to determine the temperature interval in which this process becomes intensive.

4. To explain the local drop in ductility at 330 ℃ based on an analysis of the change in lattice parameter and the precipitation of secondary phases.

2 Methods

A sheet of AA5056 alloy (ANSI H35.2) with a thickness of 3.06 mm, obtained by cold thin-sheet rolling with a relative reduction ε = 37.88%, was studied. The chemical composition of the alloy, mass %: 5.81 – Mg; 0.53 – Mn; 0.35 – Zn; 0.007 – Ti; 0.004 – Be; Al – balance.

Recrystallization annealing was carried out in a nitrogen protective gas atmosphere according to the procedure described in [3]. Annealing regimes: heating to temperatures of 290, 330, 370, 390, 470 and 530 ℃, hold of 60 minutes at each temperature, followed by furnace cooling at a rate not exceeding 5 ℃/s.

Mechanical properties were determined by static tensile testing according to ISO 6892-1:2019. Specimens were cut from the sheets in the rolling direction according to the scheme shown in Fig. 1. The tests were performed at room temperature on a Galdabini Quasar 50 universal testing machine. The mechanical properties of the initial cold-rolled samples were determined as follows: ultimate tensile strength (UTS) R_m = 464–481 MPa, yield strength $R_{p0,2}$ = 349–369 MPa, and elongation A = 9.2–10.9%.

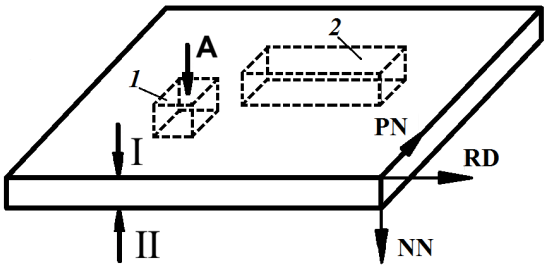


Fig. 1 Scheme of sample cutting from cold-rolled and annealed sheets: 1 – sample for X-ray studies; 2 – sample for mechanical testing; RD – rolling direction; NN – normal to the rolling plane; PN – normal lying in the rolling plane; I and II – sheet sides; A – direction for recording inverse pole figures

Texture analysis was performed using the inverse pole figure method. The measurements were taken from the sheet surface (side I in Fig. 1). The ten most intense reflections of aluminum were used: 111, 200, 220, 311, 331, 420, 422, 511, 531, 620. The pole density was calculated using formula:

$$P_{hkl} = \frac{I_{hkl}/I_{hkl\ std}}{\sum\limits_{\Delta} A_{hkl} I_{hkl}/I_{hkl\ std}}, \qquad (1)$$

where I_{hkl} is the integrated intensity of reflections from the sample under study; I_{hkl} std is the integrated intensity of reflections from a texture-free standard; A_{hkl} is the fraction of the stereographic triangle area corresponding to the reflections under study.

Normalization was carried out according to the Morris method [26]. The division of the stereographic triangle into zones for ten reflections is shown in Fig. 2.

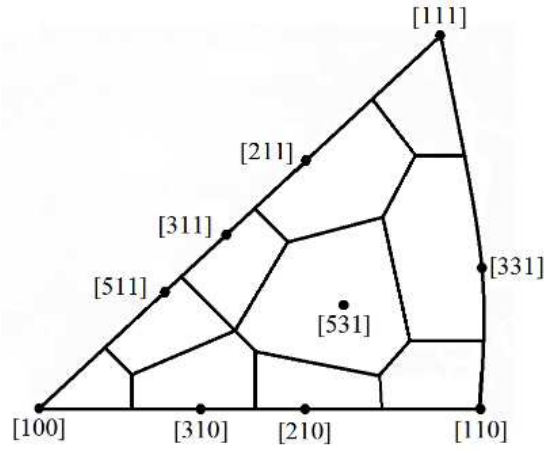


Fig. 2 Division of the stereographic triangle into zones for ten reflections of a face-centered cubic structure

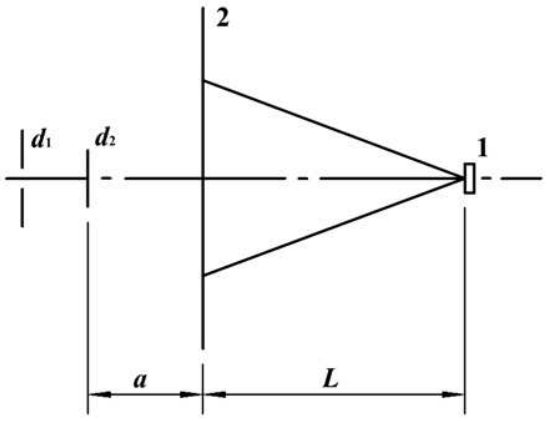


Fig. 3 Scheme of recording in the X-ray back-reflection camera: 1 – the sample under study; 2 – the X-ray film; distance a = 20 mm; distance L = 69.8 mm; input aperture d1 = 1.0 mm; output aperture d2 = 0.1 mm

It should be noted that the inverse pole figure method provides an integral characteristic of the preferential orientation of crystallographic directions parallel to the normal of the rolling plane, but does not allow one to separate the contribution of individual texture components typical for rolling of FCC metals (for example, Copper {112}<111>, S {123}<634>, and Brass {110}<112>). Therefore, the obtained inverse pole figures should be interpreted as a qualitative picture of the evolution of pole density, rather than as a precise determination of the set of components.

Diffractograms were recorded on X-ray diffractometers using CuKα radiation with a wavelength λ = 0.154178 nm. Recording conditions: Bragg–Brentano focusing [27], 2ϑ range from 16° to 70°.

To study recrystallization kinetics, the X-ray photographic method of recording Debye patterns in a back-reflection camera [24] was used, with the setup shown in Fig. 3. Recording conditions: CuKα radiation, voltage 36 kV, tube current 7 mA, exposure time 12 hours. The camera was focused at angles ϑ422 = 68°51' and ϑ511 = 81°35'. The (511) and (422) lines were recorded; the recording was performed on photographic film. The onset of primary recrystallization is indicated by the appearance of spotty reflections on continuous Debye rings, which corresponds to the presence of grains with an undistorted crystal lattice [25].

3 Results

3.1 Mechanical properties

After annealing at temperatures of 290-530 ℃ for 1 hour, the mechanical properties of the cold-rolled AA5056 sheet were determined. Fig. 4 shows the dependences of ultimate tensile strength Rm, yield strength $R_{p0.2}$, and elongation A on the annealing temperature ti. It was found that with increasing annealing temperature the values of Rm and $R_{p0.2}$ decrease monotonically, while A increases. Over the investigated temperature range, the following values were obtained: R_m = 266–442 MPa, $R_{p0.2}$ = 109–346 MPa, A = 14.8–18.7%.

Of particular interest is the non-monotonic behavior of ductility at 330 ℃: the A value decreases compared to that at 290 ℃ and then sharply increases at 370 ℃. This local drop in ductility is attributed to the precipitation of a secondary phase from the supersaturated solid solution, which leads to a decrease in the crystal lattice parameter and, consequently, to a reduction in deformability.

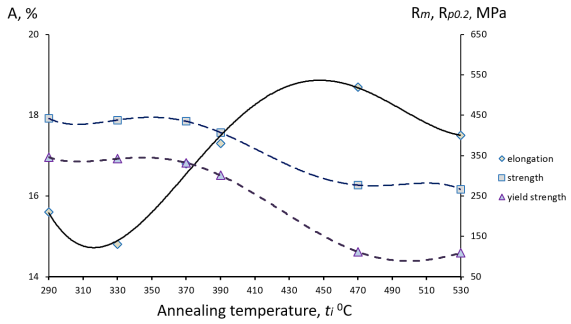


Fig. 4 Dependences of the tensile strength Rm, yield strength $R_{p0.2}$, and elongation A on the annealing temperature t_i

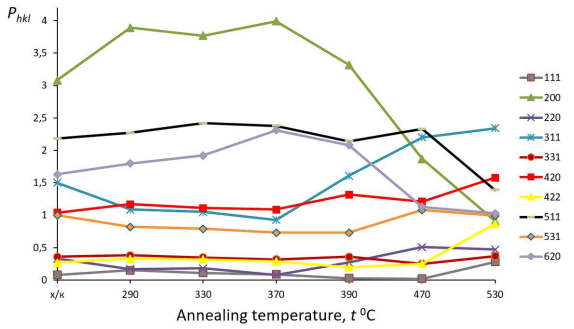


Fig. 5 Change in the pole density of the studied reflections from the surface of cold-rolled samples as a function of annealing temperature (the numbers next to the curves represent the pole density of the P_{hkl} reflections)

Based on the experimental data, regression equations were obtained, presented in Table 1. The coefficients of determination R^2 are at least 0.989, indicating a good fit. The obtained equations allow one to calculate the mechanical properties of AA5056 alloy as a function of annealing temperature in the range 290-530 °C.

Table 1 Regression equations for calculating the mechanical properties of AA5056 alloy

Parameter	Regression equation	R^2
A, %	$A = 2 \cdot 10^{-8} \cdot t_i^4 - 3 \cdot 10^{-5} \cdot t_i^3 + 0.0196 \cdot t_i^2 - 5.3941 \cdot t_i - 558.07$	0.989
R_m, MPa	$R_m = 1 \cdot 10^{-8} \cdot t_i^5 + 2 \cdot 10^{-5} \cdot t_i^4 - 0.0163 \cdot t_i^3 + 6.5226 \cdot t_i^2 - 1283.3 \cdot t_i + 99966$	1
$R_{p0.2}$, MPa	$R_{p0.2} = 6 \cdot 10^{-9} \cdot t_i^5 + 10^{-5} \cdot t_i^4 - 0.0101 \cdot t_i^3 + 4.1518 \cdot t_i^2 - 835.44 \cdot t_i + 66329$	1

Source: t_i is the annealing temperature, °C. The high R^2 values (up to 1.0) are due to interpolation with high-order polynomials; within the studied temperature range, the models provide reliable calculations.

3.2 Texture evolution

Texture analysis was performed using the inverse pole figure method. Fig. 5 shows the change in pole density Phkl for ten reflections as a function of annealing temperature. The corresponding inverse pole figures are shown in Fig. 6.

In the initial cold-rolled state and after annealing at 290 °C, the inverse pole figures exhibit an increased pole density near the <001> direction (Fig. 6, a). This may correspond either to the presence of the cube component {100}<001> or to a superposition of several deformation components (Copper, S, Brass) that contribute to this region of the stereographic triangle. According to literature data [28], for FCC metals with high stacking fault energy, the copper-type texture dominates during cold rolling, but for AA5056 alloy with high magnesium content (5.8%) deviations are possible. More precise identification of the components requires analysis of direct pole figures or orientation distribution functions. After annealing in the range of 330-390 °C, the cube texture component remains dominant (Fig. 6, b).

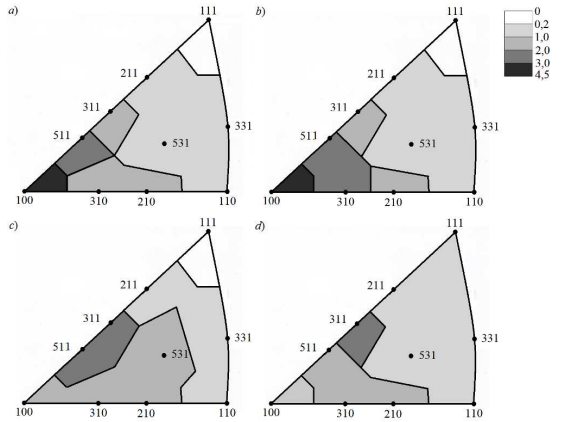


Fig. 6 Inverse pole figures most characteristic of the surface of Al–Mg alloy samples: a) – initial cold-rolled state (without annealing) and after annealing at t_i = 290 ℃; b) – after annealing in the temperature range t_i = 330-390 ℃; c) – after annealing at t_i = 470 ℃; d) – after annealing at t_i = 530 ℃)

When the annealing temperature is raised to 470 ℃, a change in the texture state occurs. The predominant orientations become the rather unusual A/rot. W {511}<110> component [29] and the silver orientation {311}<211> (Fig. 6, c). At 530 ℃, the {311}<211> component remains dominant (Fig. 6, d). Such a texture change is associated with the development of primary and secondary recrystallization, as well as with the influence of manganese dispersoids, which suppress the growth of some orientations and promote the development of others.

3.3 Recrystallization kinetics (X-ray photographic method)

To study the onset and development of primary recrystallization, the X-ray photographic method of recording Debye patterns was used. Fig. 7 shows a Debye pattern of the initial cold-rolled sample: the (511) and (422) Debye rings are diffuse, which is typical for a work-hardened state with a high level of microdistortions and small crystallite sizes.

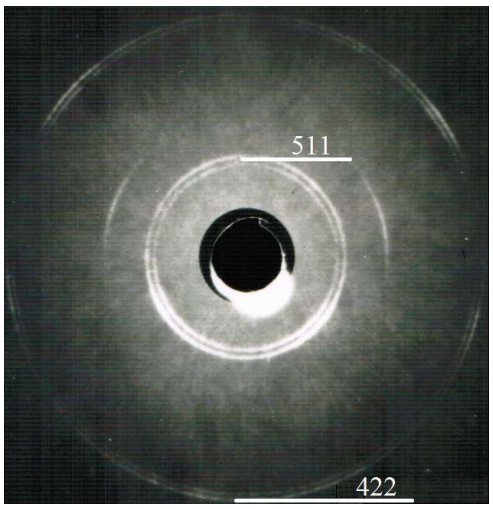


Fig. 7 Debye pattern of the surface of the initial cold-rolled AA5056 alloy sample

Fig. 8 shows sector X-ray diffraction patterns of samples after annealing at different temperatures. After annealing at 290 ℃and 330 ℃(Fig. 8, a, b), the Debye rings remain continuous and fairly sharp; however, at 330 ℃a decrease in the diameter of the (511) ring is observed, which indicates a reduction in the lattice parameter due to the precipitation of a secondary phase.

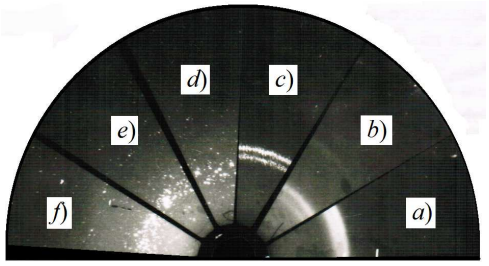


Fig. 8 Sector X-ray diffraction patterns of the surface of cold-rolled annealed Al–Mg alloy samples: a) – annealing at t_i = 290 ℃; b) – annealing at t_i = 330 ℃; c) – annealing at t_i = 370 ℃; d) – annealing at t_i = 390 ℃; e) – annealing at t_i = 470 ℃; f) – annealing at t_i = 530 ℃

Upon annealing at 370 ℃ (Fig. 8, c), small spotty reflections begin to appear on the continuous rings. This indicates the nucleation of the first recrystallized grains with an undistorted crystal lattice. The appearance of spotty reflections was

recorded at 370 ℃, which allows this temperature to be taken as the onset of primary recrystallization for the alloy under study at a reduction of 37.9%.

4 Discussion

The obtained results allow us to establish the relationship between the annealing temperature, mechanical properties, texture and recrystallization kinetics of AA5056 alloy.

The onset of recrystallization at 370 ℃, recorded by the X-ray photographic method, is 40-50 ℃ higher than for pure aluminum under similar deformation. This is explained by the inhibiting effect of magnesium (solute drag effect) and manganese dispersoids, which delay the movement of grain and subgrain boundaries [7, 12]. The local decrease in ductility at 330 ℃is associated with the decomposition of the supersaturated solid solution and the formation of clusters or metastable phases, which reduces the lattice parameter and temporarily lowers the deformability. At 370 ℃, these phases dissolve, the lattice parameter is restored, and recrystallization begins, leading to a sharp increase in ductility.

The preservation of the cube texture {100}<001> up to 390 ℃ indicates that primary recrystallization at these temperatures does not lead to a complete change in orientations. Only after the completion of recrystallization and at higher temperatures (470-530 ℃) does secondary recrystallization or selective grain growth with {311}<211> and {511}<110> orientations occur, which is consistent with literature data for Al–Mg alloys with Mn additions [9, 14].

Thus, the combination of mechanical testing, texture analysis and X-ray Debye pattern recording makes it possible to fully characterize the recrystallization process and to recommend optimal annealing regimes for AA5056 alloy: for maximum ductility – annealing at 370-390 ℃, for maintaining increased strength – annealing not higher than 330 ℃.

5 Conclusions

Based on the conducted study of the effect of annealing temperature in the range of 290-530 ℃ with a holding time of 1 hour on the mechanical properties, texture and primary recrystallization kinetics of a cold-rolled AA5056 alloy sheet (reduction 37.9%, thickness 3.06 mm, magnesium content

1. It was found that with increasing annealing temperature, the ultimate tensile strength R_m and yield strength $R_{p0.2}$ regularly decrease from 464–481 MPa and 349–369 MPa in the cold-rolled state to 266–442 MPa and 109–346 MPa after annealing at 530 ℃, respectively, while the elongation A increases from 9.2–10.9% to 17.5%. Regression equations ($R^2 = 0.989$) were obtained, allowing a quantitative description of these dependences in the studied temperature range.

2. Analysis of inverse pole figures showed that in the cold-rolled state and after annealing up to 390 ℃, the maximum pole density corresponds to the <001> direction. After annealing at 470 ℃and above, the preferred orientation shifts towards the {311}<211> and {511}<110> components.

3. Using the X-ray photographic method of recording Debye patterns, the onset of primary recrystallization was recorded for the first time for AA5056 alloy by the appearance of spotty reflections on the (511) and (422) Debye rings at a temperature of 370 ℃. At 330 ℃, a local decrease in ductility was found, explained by the precipitation of a secondary phase from the supersaturated solid solution and a decrease in the crystal lattice parameter.

4. The recommended annealing regimes for AA5056 alloy after cold rolling with a reduction of about 38% are: for achieving maximum ductility, annealing at 370-390 ℃; for maintaining increased strength, annealing not higher than 330 ℃. The obtained regression equations can be used to predict mechanical properties when assigning heat treatment to rolled sheet from Al–Mg system alloys.

Declarations

- **Funding**
  The authors declare that no funds, grants, or other support were received during the preparation of this manuscript.
- **Conflict of interest/Competing interests (check journal-specific guidelines for which heading to use)**

The authors have no relevant financial or non-financial interests to disclose.

- **Ethics approval**
  Not applicable. This research did not involve human participants or animals.
- **Consent**
  Not applicable. This study did not involve human participants.
- **Data**
  All data supporting the findings of this study are included in this published article (and its supplementary information files).
- **Material**
  The AA5056 (ANSI H35.2) aluminium–magnesium alloy with high magnesium content investigated in this work is available from the corresponding author upon reasonable request for non-commercial research purposes
- **Code availability**
  Figures 1, 2, 3 and 6 were drawn using Microsoft Paint. Figures 4 and 5 were generated with Microsoft Excel. Text annotations in Figures 7 and 8 were added using Microsoft Paint. Standard commercial and open-source software was used for data analysis.
- **Author contribution**
  All authors contributed to the study conception and design. Material preparation, data collection and analysis were performed by Ivan D. Pospelov, Andrey A. Nikiforov, Natalia L. Bolobanova, Sergey A. Pyatkovsky and Zoya M. Malkova. The first draft of the manuscript was written by Ivan D. Pospelov and all authors commented on previous versions of the manuscript. All authors read and approved the final manuscript.

References

1. Skripalenko MM, Rogachev SO, Skripalenko MN, Andreev VA, Karelin RD, Yusupov VS, Cheverikin VV, Romantsev BA, Danilin AV (2025) Estimation of deformation zone parameters and their influence on microstructure and properties formation of aluminum strip while cold rolling. J Mater Eng Perform 34:26509–26519. https://doi.org/10.1007/s11665-025-12920-w

2. Konstantinov IL, Baranov VN, Sidelnikov SB, Kulikov BP, Bezrukikh AI, Frolov VF, Orelkina TA, Voroshilov DS, Yuryev PO, Belokonova IN (2020) Investigation of the structure and properties of cold-rolled strips from experimental alloy 1580 with a reduced scandium content. Int J Adv Manuf Technol 109:443–450. https://doi.org/10.1007/s00170-020-05681-4

3. Pospelov ID, Matveeva DV, Smirnov AV (2025) Study of mechanical properties and structure of steel C70D after drawing deformation and spheroidizing annealing. Met Sci Heat Treat 66:531–535. https://doi.org/10.1007/s11041-025-01082-0

4. Matvija M, Fujda M, Milkovič O, Vojtko M, Gáborová K (2025) Thermal stability of the ultrafine-grained structure and mechanical properties of AlSi7MgCu0.5 alloy processed by equal channel angular pressing at room temperature. Crystals 15(8):701. https://doi.org/10.3390/cryst15080701

5. Yu Q-B, Sun Y, Yang G-X, Zhao Y-J, Zhang M-D, Liu X-H (2013) Thermal effect on recrystallization of cold-deformed aluminium alloy and its mechanisms. Trans Mater Heat Treat 34(9):42–46

6. Rokhlin LL, Bochvar NR, Lysova EV, Leonova NP, Korolkova IG (2008) Phase equilibria in the ternary Al-Sc-Mn system. Russ Metall (Metally) 2008(1):84–88. https://doi.org/10.1134/S0036029508010163

7. Qian X, Parson N, Chen X-G (2020) Effects of Mn content on recrystallization resistance of AA6082 aluminum alloys during post-deformation annealing. J Mater Sci Technol 52(1):189–197. https://doi.org/10.1016/j.jmst.2020.04.015

8. Li Y, Qian X, Zhang Y et al (2021) Analysis on the hot deformation flow stress curves of novel 6082 aluminium alloys with Mn addition. IOP Conf Ser: Mater Sci Eng 1133:012007. https://doi.org/10.1088/1757-899X/1133/1/012007

9. Elasheri A, Ghosh A, Parson N, Chen X-G (2025) Microstructure and texture evolution during extrusion of 6xxx aluminum alloys with Mn/Zr additions. J Mater Sci 60:22252–22269. https://doi.org/10.1007/s10853-025-11646-3

10. Farsadhemmati S, Shaban Ghazan M, Eghbali B (2025) Effect of post-deformation annealing on the microstructure and mechanical properties of AA6061/AA1050 laminated composite processed by accumulative roll bonding. Metallogr Microstruct Anal 14:946–958. https://doi.org/10.1007/s13632-025-01209-2

11. Aryshenskii E, Drits A, Konovalov S et al (2025) Impact of the strain rate and grain size

on the intensification or mitigation of the serrated flow behavior presented in commercial 5182 and 1565Ch Al-Mg alloys. J Mater Eng Perform 34:26509–26519. https://doi.org/10.1007/s11665-025-11217-2

12. Algendy AY, Liu K, Chen X-G (2023) Effect of Mn-bearing dispersoids on tensile properties and recrystallization resistance of Al-3Mg-0.8Mn rolled alloy. Adv Eng Mater 25(19):2300667. https://doi.org/10.1002/adem.202300667

13. Matvija M, Fujda M, Milkovič O et al (2017) Phase analysis of EN AW 6023 aluminum alloy after short time aging. Manuf Technol 17(6):912–916. https://doi.org/10.21062/ujep/x.2017/a/1213-2489/MT/17/6/912

14. Liu F, Zhu X, Qin J et al (2022) Effect of Mn/Cr ratio on precipitation behaviors of α-Al(FeMnCr)Si dispersoids and mechanical properties of Al–Mg–Si–Cu alloys. Mater Sci Eng A 860:144269. https://doi.org/10.1016/j.msea.2022.144269

15. Šlapáková M, Kihoulou B, Grydin O (2023) Development of microstructure of asymmetrically rolled AA3003 aluminium sheets with Zr addition. J Alloys Metall Syst 2(2):100012. https://doi.org/10.1016/j.jalmes.2023.100012

16. Bakr A, Rometsch P, Chen X-G (2025) Effect of Sc and Zr microalloying on recrystallization behavior of 1xxx aluminum heat exchanger alloys during post-deformation annealing. J Mater Sci: Mater Eng 20:84. https://doi.org/10.1007/s10853-025-11855-8

17. Riddle YW, Sanders TH (2000) Recrystallization performance of AA7050 varied with Sc and Zr. Mater Sci Forum 331–337:799–804. https://doi.org/10.4028/www.scientific.net/MSF.331-337.799

18. Forbord B, Hallem H, Marthinsen K (2004) The effect of Sc on the extrudability and recrystallisation resistance of Al-Mn-Zr-alloys. Mater Sci Forum 467–470:369–374. https://doi.org/10.4028/www.scientific.net/MSF.467-470.369

19. Gordeeva MI, Betsofen SYa, Shalin AV, Ogolodkov MS, Ogolodkova YuS, Wu R, Maksimenko EI, Prokopenko DA (2024) Influence of the phase composition and texture on the elastic properties of Al–Cu–Li alloys. Russ Metall (Metally) 2024(2):423–430. https://doi.org/10.1134/S0036029524700745

20. Slámová M, Ocenasek V, Vander Voort GF (2003) Polarized light microscopy - an essential method for the investigation of the recrystallization of aluminum alloys. Microsc Microanal 9(S2):544. https://doi.org/10.1017/S1431927603035759

21. Liu R, Zhang Z, Zhou G et al (2026) A novel cellular automaton for simulating static recrystallization of aluminum alloys incorporating both solute drag and particle effects. Adv Manuf. https://doi.org/10.1007/s40436-025-00578-5

22. Liu WC, Yuan H, Huang MJ, Cai DY, Yang QX (2009) Quantifying the recrystallization of cold rolled AA 3015 aluminum alloy by X-ray diffraction. Mater Sci Eng A 524(1–2):168–175. https://doi.org/10.1016/j.msea.2009.07.031

23. Lukin EI, Ashmarin AA, Bannykh IO et al (2023) Effect of the reduction during cold rolling on the phase composition, texture, and residual stresses in 20Kh15AN3MD2 steel. Russ Metall (Metally) 2023(11):1598–1605. https://doi.org/10.1134/S0036029523110101

24. Sharma SK (ed) (2011) X-ray spectroscopy. InTech, Croatia. https://doi.org/10.5772/1422

25. Uzun F, Daisenberger D, Liogas K, Wang ZI, Chen J, Besnard C, Korsunsky AM (2024) Extended caking method for strain analysis of polycrystalline diffraction Debye–Scherrer rings. Crystals 14(8):716. https://doi.org/10.3390/cryst14080716

26. Stepanenko AV (2021) A study of angular distributions of crystallites in polycrystals with hcp-structure. Int Res J (103):139–144. https://doi.org/10.23670/IRJ.2021.103.1.021

27. Huang J, Tornheim AP, Shi X, Wolfman M, Chen Y, Heald MS, Kelly SD, Sterbinsky GE (2025) Dispersive X-ray absorption spectroscopy using independent grazing incidence focusing and convexly bent Bragg crystal dispersing optics. J Synchrotron Radiat 32(4):1068–1084. https://doi.org/10.1107/S160057752500325X

28. Gupta A, Kumar R, Kaushik L, Shukla S, Tandon V, Choi S-H (2024) Microstructure and texture evolution in thermomechanically processed FCC metals and alloys: a review. Korean J Met Mater 62(7):564–592. https://doi.org/10.3365/KJMM.2024.62.7.564

29. Hirsch J, Lücke K (1988) Description and presentation methods for

textures. Textures Microstruct 8–9:131–151.
https://doi.org/10.1155/TSM.8-9.131